

# Controlling plasmonic hot-spots by interfering Airy beams

Angela E. Klein,<sup>1,\*</sup> Alexander Minovich,<sup>2</sup> Michael Steinert,<sup>1</sup> Norik Janunts,<sup>1</sup> Andreas Tünnermann,<sup>1,3</sup> Dragomir N. Neshev,<sup>2</sup> Yuri S. Kivshar,<sup>2</sup> and Thomas Pertsch<sup>1</sup>

<sup>1</sup>*Institute of Applied Physics, Abbe Center of Photonics, Friedrich-Schiller-Universität Jena, 07743 Jena, Germany*

<sup>2</sup>*Nonlinear Physics Centre and Centre for Ultrahigh-bandwidth Devices for Optical Systems (CUDOS), Research School of Physics and Engineering, The Australian National University, ACT 0200, Canberra, Australia*

<sup>3</sup>*Fraunhofer Institute of Applied Optics and Precision Engineering, 07745 Jena, Germany*

\*Corresponding author: [angela.klein@uni-jena.de](mailto:angela.klein@uni-jena.de)

Compiled June 29, 2012

We predict and demonstrate the generation of a plasmonic hot-spot on the surface of a metal film by the interference of two Airy surface plasmons. We show that the position of the hot-spot can be controlled by the distance between the excitation gratings, as well as by the phase front of the initial excitation. The observed effect constitutes a planar analogy to Airy beam autofocusing and offers new opportunities for spatially-resolved surface plasmon sensing and optical surface tweezers. © 2012 Optical Society of America

OCIS codes: 240.6680, 050.1940, 350.5500

Non-diffracting beams have been the subject of many theoretical [1, 2] and experimental [3–6] studies in optics since their first description in 1979 [7]. Diffraction-free solutions of the wave equation comprise the well-known Bessel, Mathieu and Airy beams. However in (1+1)D systems, Airy waves represent the only possible non-spreading solution. Airy beams can propagate diffraction-free on a two-dimensional surface, e.g. they can be realized in the form of a surface plasmon polariton (SPP) wave packet [8]. Recently plasmonic Airy beams have been demonstrated experimentally with different methods for excitation [9–11]. While being by nature non-paraxial beams [9], Airy plasmons also demonstrate a number of remarkable properties similar to their 3D counterparts: they do not diffract within their diffraction free zone, they self-accelerate during propagation, and they recover their shape after passing through obstacles. In addition to the unique properties of non-diffracting beams in free space, Airy surface plasmons tightly confine energy near the metal-air interface. These properties make Airy waves attractive for plasmonic circuitry applications and surface manipulation of nano-objects [12].

Indeed, due to the self-acceleration of the Airy plasmons they can be used to guide small dielectric particles along a parabolic trajectory on the metal surface. Nevertheless, they cannot be directly utilized for the creation of localized hot-spots on the surface, which would enable additional applications in microscopy, optical data storage and biosensing as recently attempted experimentally through spatial coherent control [13, 14]. In this work we predict theoretically and demonstrate experimentally that the interference of two mirror-symmetric Airy plasmons results in the formation of a single localized hot-spot on the surface. Furthermore, we show that the position and existence of the generated hot-spot can be controlled by displacing the excitation gratings or by simple phase modulation of the input coupling beam.

Importantly, the observed interference of the two Airy

plasmons represents the two-dimensional analogue of the earlier predicted effect of Airy beam autofocusing [15]. In the Airy autofocusing process a radially symmetric (in the transverse plane) Airy beam is shown to exhibit focusing to a single point, demonstrating up to three orders of magnitude field enhancement in the focal region. In the context of SPPs, this auto-focusing effect occurs just in a single plane.

In our experiments we use gratings in the form of rectangular slits in a metal layer to excite surface plasmons (Fig. 1). The grating period along the  $z$  axis corresponds to the surface plasmon wavelength, so that SPPs propagating along the  $z$ -axis are excited when the gratings are illuminated at normal incidence ( $\alpha = 0^\circ$ ) with a beam polarized along the  $z$  axis. Now the grating is subdivided into columns in the  $x$ -direction. By selectively shifting the columns along the SPP propagation direction ( $z$  axis), the phase of the plasmonic wave packet can be spatially modulated. Phase variations of  $\pi$  are achieved by shifting every second column by half a grating period with respect to the neighboring columns [Fig. 1(d)]. The widths of the columns are chosen to match the zeros of Airy pattern amplitude, as shown in [Fig. 1(b) and (c)]. The generation technique is similar to our previous work on excitation of single Airy plasmons [9], however by placing two excitation gratings side by side and illuminating them simultaneously, two Airy wave packets are generated.

Our sample was fabricated on a 150 nm thick gold film deposited on a glass substrate by dc sputtering. With a Focused Ion Beam (FIB), the metal was completely removed from the areas forming the rectangular slit pattern of the excitation gratings. A number of grating patterns comprising 10 columns per grating and having different separation distances  $d$  were prepared. The gratings were illuminated from the substrate side by a cw diode laser with a free-space wavelength of 784 nm. The beam was weakly focused to a focal spot of  $\sim 50 \mu\text{m}$ .

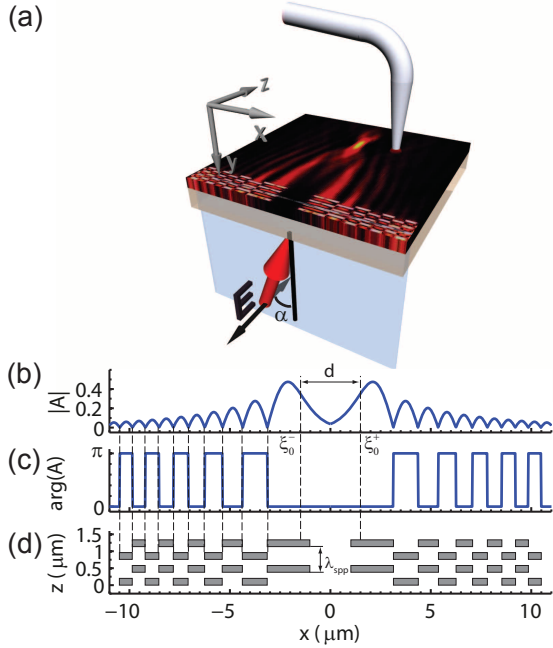


Fig. 1. Excitation and interference of Airy plasmons: (a) Schematic of the experimental setup with the mirror symmetric gratings. Rectangular slits are arranged in 10 columns per grating with varying width along  $x$  direction. Along  $z$  direction, the gratings comprise 11 periods and the slits are 200 nm wide. The gratings are illuminated from the substrate side by a broad Gaussian beam with  $\lambda = 784$  nm and polarization along  $z$ . (b, c) Absolute value and phase of the amplitude function of the two Airy plasmons. The main lobe half width is  $x_0 = 700$  nm.  $\xi_0^-$  ( $\xi_0^+$ ) denotes the  $x$ -coordinate where the argument of the left (right) Airy function becomes zero. (d) Grating geometry for excitation of Airy plasmons.  $\lambda_{\text{SPP}} = 764$  nm denotes the SPP wavelength. The distance between the gratings,  $d$ , is measured between  $\xi_0^-$  and  $\xi_0^+$ .

Collection-mode scanning near-field optical microscopy (SNOM, Nanonics Imaging MV-4000) with a gold-coated fiber probe (aperture diameter: 150 nm) was used to map the resulting interference pattern in the near-field. The optical signal was detected by a SPCM-AQR-14 (Perkin-Elmer) single photon counting module.

In a first series of measurements, we use two excitation gratings in a mirror-symmetric configuration. Each grating excites an Airy plasmon. As the main lobes of both Airy plasmons follow parabolic trajectories, they collide on the symmetry axis of the structures, generating a bright hot-spot due to their interference. In Fig. 2 we present a comparison between our FDTD simulations (a-c) and experimental results (e-g) for different distances between both excitation gratings, showing good agreement between numerical simulation and measured field maps. An important observation is that as the distance between the gratings increases, the bright hot-spot shifts along the  $z$  axis and moves away from the gratings. Due to losses during plasmon propagation, the intensity profiles of the main lobes change during propagation. Consequently, the size and intensity of the spot also vary. In the simulations we obtain a Full Width Half Maximum

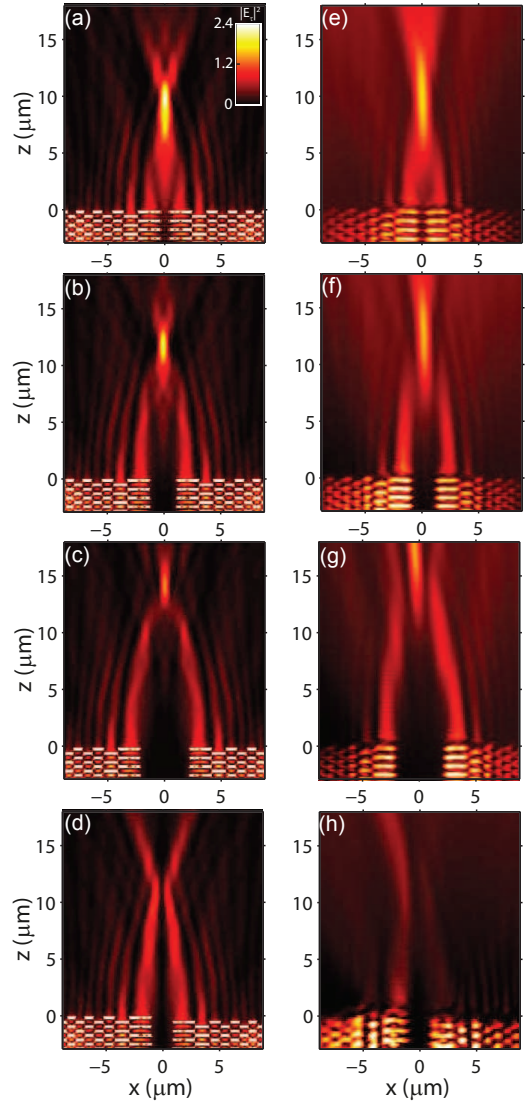


Fig. 2. Square of the modulus of the tangential component of the electric field  $|E_\tau|^2$ , where  $E_\tau$  is the component of the electric field parallel to the sample plane, calculated by FDTD and evaluated 10 nm above the sample surface (a-d) and measured by SNOM (e-h), for different separation distances  $d = 1.5 \mu\text{m}$  (a,e),  $d = 3.0 \mu\text{m}$  (b,f), and  $d = 5.0 \mu\text{m}$  (c,g). The illumination intensity  $|E_\tau|^2$  in the FDTD calculations is 1. (d,h) were obtained for a separation distance  $d = 2.5 \mu\text{m}$  and a  $z$ -shift of half a grating period (out-of-phase excitation). The movie (Media 1) shows simulated data for continuously increasing  $z$ -shift.

size of the hot-spot as small as  $0.5 \mu\text{m}$  by  $1.5 \mu\text{m}$  in the  $x$ - and  $z$ -direction, respectively. Around 3% of the energy of the laser beam is coupled into Airy plasmons propagating in positive  $z$  direction. For a grating distance  $d = 3.0 \mu\text{m}$ , approximately 20% of this energy reaches the hot spot, so that the overall coupling efficiency to the hot spot is 0.6%. The intensity of the focal spot is up to 2.4 times higher than the illumination intensity (Fig. 2(a)).

In the experiments the hot-spots of the interfering Airy plasmons are slightly wider than in the simula-

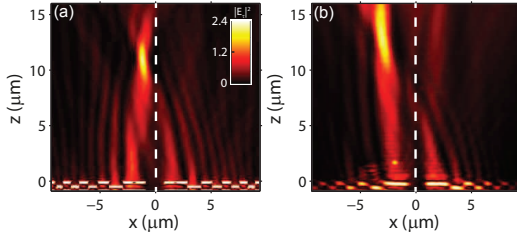


Fig. 3. Tangential component of the electric field ( $|E_\tau|^2$ ) calculated by FDTD (a) and measured by SNOM (b) for tilted illumination at  $\alpha = 5.0^\circ$  (a) and  $5.3^\circ \pm 0.3^\circ$  (b), for  $d = 2.5 \mu\text{m}$ . The dashed line marks the symmetry axis. The illumination intensity  $|E_\tau|^2$  in the FDTD calculation is 1.

tions. This is attributed to the non-negligible effect of the SNOM tip on the propagation of the Airy plasmons.

Importantly, by shifting one of the gratings along the  $z$  direction and thus breaking the mirror symmetry of the sample, a phase shift between the generated Airy plasmons can be introduced. The phase shift influences the brightness of the focal spot, as constructive and destructive interference between both main lobes alternate when the shift continuously increases (see Fig. 2(d) and (h), Media 1). Fig. 2(d) and (h) demonstrate the effect of shifting one grating by half a period, corresponding to a phase shift of  $\pi$ , for a grating distance  $d = 2.5 \mu\text{m}$ . This leads to a dramatically different interference pattern. Instead of interfering constructively and creating a bright spot, both main lobes now interfere destructively and no hot-spot can be observed, as both the numerical simulation and the measured field map demonstrate. Our simulations show that for a shift of a whole grating period, corresponding to a phase shift of  $2\pi$ , the focus reappears having a brightness and a shape similar to the initial picture.

For applications like addressing of absorbing particles at different positions on the surface, it is of particular interest to dynamically shift the position of the bright hot-spot. This can be easily achieved by tilting the illuminating beam sideways [see Fig. 1(a)], thus introducing an additional momentum  $k_x$  and breaking the mirror symmetry of the setup. As a result, the bright hot-spot shifts sideways. For a grating with a separation distance  $d = 2.5 \mu\text{m}$ , FDTD simulations predict that an illumination angle of  $\alpha = 5^\circ$  at the glass/gold interface causes the focal spot to shift by  $1.3 \mu\text{m}$  along the  $x$ -direction and for the angle of  $\alpha = 10^\circ$  the spot is laterally shifted by  $2.3 \mu\text{m}$ . Fig. 3(a) shows the numerical simulation for an incidence angle of  $5^\circ$ . For the SNOM image in Fig. 3(b), the angle of incidence of the excitation beam was chosen so that after refraction at the air/glass interface of the substrate rear side, the grating was illuminated at an angle  $\alpha = 5.3^\circ \pm 0.3^\circ$ . This leads to a shift of the maximum of the interference pattern by  $3.0 \mu\text{m}$ . The FWHM of the bright hot-spot remains below  $1 \mu\text{m}$  in  $x$ -direction. The lateral shift of the spot corresponds thus to three FWHMs and is significantly larger than expected from the simulation. This dynamic shift

could serve to serially address nanoparticles, molecules or other structures of interest at different positions on the metal surface.

In conclusion, we have studied experimentally and numerically the interference pattern of Airy plasmons. We have observed the formation of a strong focal hot-spot at the intersection of main lobes of the two Airy plasmons. In contrast to hot-spots created with the help of nanoantennas, no structuring of the sample in the close vicinity of the bright spot is necessary. Our scheme is also significantly simpler than the schemes based of coherent spatial control used previously [13, 14], where superposition of more than two beams with specially engineered phase is required to create a single hot-spot. Finally, we have shown that tilting of the incident beam causes a shift of the intensity maximum in lateral direction. We believe that the described interference properties may be useful for plasmonic circuitry applications, surface optical tweezers, optical data storage, and biosensing.

We acknowledge support from the German Research Foundation (SPP 1391 and JSMC), German federal Ministry of Education and Research (PhoNa) and the Thuringian Ministry of Education Science and Culture (MeMa), the Australian Research Council, the Go8-DAAD Joint Research Cooperation Scheme, and the Australian National Computational Infrastructure.

## References

1. J. Durnin, *J. Opt. Soc. Am. A* **4**, 651 (1987).
2. J. C. Gutiérrez-Vega, M. D. Iturbe-Castillo, and S. Chávez-Cerda, *Opt. Lett.* **25**, 1493 (2000).
3. J. Durnin, J. J. Miceli, and J. H. Eberly, *Phys. Rev. Lett.* **58**, 1499 (1987).
4. Y. Lin, W. Seka, J. H. Eberly, H. Huang, and D. L. Brown, *Appl. Opt.* **31**, 2708 (1992).
5. G. A. Siviloglou, J. Broky, A. Dogariu, and D. N. Christodoulides, *Phys. Rev. Lett.* **99**, 213901 (2007).
6. J. Broky, G. A. Siviloglou, A. Dogariu, and D. N. Christodoulides, *Opt. Express* **16**, 12880 (2008).
7. M. V. Berry and N. L. Balazs, *Am. J. Phys.* **47**, 264 (1979).
8. A. Salandrino and D. N. Christodoulides, *Opt. Lett.* **35**, 2082 (2010).
9. A. Minovich, A. E. Klein, N. Janunts, T. Pertsch, D. N. Neshev, and Y. S. Kivshar, *Phys. Rev. Lett.* **107**, 116802 (2011).
10. P. Zhang, S. Wang, Y. Liu, X. Yin, C. Lu, Z. Chen, and X. Zhang, *Opt. Lett.* **36**, 3191 (2011).
11. L. Li, T. Li, S. M. Wang, C. Zhang, and S. N. Zhu, *Phys. Rev. Lett.* **107**, 126804 (2011).
12. M. Righini, A. Zelenina, C. Girard, and R. Quidant, *Nature Phys.* **3**, 477 (2007).
13. T. S. Kao, S. D. Jenkins, J. Ruostekoski, and N. I. Zheludev, *Phys. Rev. Lett.* **106**, 085501 (2011).
14. B. Gjonaj, J. Aulbach, P. M. Johnson, A. P. Mosk, L. Kuipers, and A. Lagendijk, *Nature Photon.* **5**, 360 (2011).
15. N. K. Efremidis and D. N. Christodoulides, *Opt. Lett.* **35**, 4045 (2010).

## Informational Fourth Page

### References with titles

1. J. Durnin, "Exact solutions for nondiffracting beams. I. The scalar theory," *J. Opt. Soc. Am. A* **4**, 651–654 (1987).
2. J. C. Gutiérrez-Vega, M. D. Iturbe-Castillo, and S. Chávez-Cerda, "Alternative formulation for invariant optical fields: Mathieu beams," *Opt. Lett.* **25**, 1493–1495 (2000).
3. J. Durnin, J. J. Miceli, and J. H. Eberly, "Diffraction-free beams," *Phys. Rev. Lett.* **58**, 1499–1501 (1987).
4. Y. Lin, W. Seka, J. H. Eberly, H. Huang, and D. L. Brown, "Experimental investigation of bessel beam characteristics," *Appl. Opt.* **31**, 2708–2713 (1992).
5. G. A. Siviloglou, J. Broky, A. Dogariu, and D. N. Christodoulides, "Observation of accelerating airy beams," *Phys. Rev. Lett.* **99**, 213901 (2007).
6. J. Broky, G. A. Siviloglou, A. Dogariu, and D. N. Christodoulides, "Self-healing properties of optical airy beams," *Opt. Express* **16**, 12880–12891 (2008).
7. M. V. Berry and N. L. Balazs, "Nonspreading wave packets," *American Journal of Physics* **47**, 264–267 (1979).
8. A. Salandrino and D. N. Christodoulides, "Airy plasmon: a nondiffracting surface wave," *Opt. Lett.* **35**, 2082–2084 (2010).
9. A. Minovich, A. E. Klein, N. Janunts, T. Pertsch, D. N. Neshev, and Y. S. Kivshar, "Generation and near-field imaging of airy surface plasmons," *Phys. Rev. Lett.* **107**, 116802 (2011).
10. P. Zhang, S. Wang, Y. Liu, X. Yin, C. Lu, Z. Chen, and X. Zhang, "Plasmonic airy beams with dynamically controlled trajectories," *Opt. Lett.* **36**, 3191–3193 (2011).
11. L. Li, T. Li, S. M. Wang, C. Zhang, and S. N. Zhu, "Plasmonic airy beam generated by in-plane diffraction," *Phys. Rev. Lett.* **107**, 126804 (2011).
12. M. Righini, A. Zelenina, C. Girard, and R. Quidant, "Parallel and selective trapping in a patterned plasmonic landscape," *Nature Physics* **3**, 477–480 (2007).
13. T. S. Kao, S. D. Jenkins, J. Ruostekoski, and N. I. Zheludev, "Coherent Control of Nanoscale Light Localization in Metamaterial: Creating and Positioning Isolated Subwavelength Energy Hot Spots," *Phys. Rev. Lett.* **106**, 085501 (2011).
14. B. Gjonaj, J. Aulbach, P. M. Johnson, A. P. Mosk, L. Kuipers, and A. Lagendijk, "Active spatial control of plasmonic fields," *Nature Photon.* **5**, 360–363 (2011).
15. N. K. Efremidis and D. N. Christodoulides, "Abruptly autofocusing waves," *Opt. Lett.* **35**, 4045–4047 (2010).